13th Australasian Fluid Mechanics Conference
Monash University, Melbourne, Australia
13-18 December 1998

SHEAR LAYERS DRIVEN BY TURBULENT PLUMES

Alan B. D. WONG and Ross W. GRIFFITHS
Research School of Earth Sciences,
The Australian National University, Canberra, ACT 0200, Australia

ABSTRACT

A turbulent plume from a continuous source of buoyancy in a wide tank is shown to generate a series of counterflowing horizontal shear layers throughout the tank (figure 1). These layers are supported by the stable density stratification produced by the plume and are superimposed on the vertical advection and entrainment inflow which make up the so-called "filling-box" circulation of Baines and Turner (1969). Thus at some depths the surrounding water flows away from the plume instead of being entrained, although we see no evidence of 'detrainment' of dense plume water. Given the stratification produced by the plume at large times, the time scale for the velocity structure to adjust to changes in forcing is proportional to the time for long internal gravity waves to travel the length of the tank. The shear layers are interpreted in terms of the internal normal modes, with the sixth, seventh and eighth baroclinic modes dominant.

INTRODUCTION

Most studies of turbulent buoyant plumes have focused on the plume flow itself, with associated motions outside the plume assumed to be small. In this paper, we report experiments which show that in long tanks, a series of strong counterflowing shear layers is established in the stratification produced by the "filling-box" mechanism (Wong and Griffiths, 1998). We present evidence that the layers are produced by internal gravity wave normal modes which are excited by the plume outflow.

BACKGROUND

The "filling-box" analysis of Baines and Turner (1969) predicts the properties of a buoyant plume and the density stratification produced in a finite environment. It assumes that buoyancy-driven convection is the dominant transport mechanism in the plume and that, far away from the plume, the only motions are those of passive advection.

Dense water produced at a buoyancy source generates a turbulent buoyant plume. During its descent the plume entrains surrounding water and increases in radius and decreases in density. The outflow from the plume as it strikes the bottom enters the envrionment to generate a vertical advection that fills the box with dense water. The plume entrains

Figure 1. Photograph of the shear layers generated by a plume. Potassium permanganate crystals dropped into the tank left an initially vertical line of dissolved dye. The passive movement of this dye line reveals the shear layers.

back some of the dense water and the outflow becomes progressively denser. This establishes a stable stratification through the box.

Let ρ_p, R and W be the density, radius and vertical (downward) velocity of the plume respectively, ρ_e the density of the surrounding water, ρ_r a reference density (taken to be that of the environment water at the source level) and V the vertical velocity in the environment, with t the time and z the vertical coordinate (origin at depth of source). We assume a top-hat profile in which the plume properties are constant across a horizontal cross-section. The equations representing the conservation of volume, momentum and mass deficiency are

$$\frac{d}{dz}\left(\pi R^2 W\right) = 2\pi ERW,$$

$$\frac{d}{dz}\left(\pi R^2 W^2 \rho_p\right) = \pi R^2 g\left(\rho_p - \rho_e\right) \qquad (1)$$

and

$$\frac{d}{dz}\left[\pi R^2 W\left(\rho_p - \rho_r\right)\right] = 2\pi ERW\left(\rho_e - \rho_r\right),$$

while equations representing conservation of volume and density in the environment are

$$AV = -\pi R^2 W$$

and (2)

$$\frac{d}{dt}\left(g\frac{\rho_e - \rho_r}{\rho_r}\right) = V\frac{d}{dz}\left(g\frac{\rho_e - \rho_r}{\rho_r}\right).$$

Here, E (≈ 0.129) is the experimentally determined entrainment coefficient (Turner, 1986), g is the gravitational acceleration and A is the horizontal cross-sectional area of the box.

Baines and Turner (1969) described solutions to (1) and (2) for large times. A typical stratification in the environment at large times is given in figure 2.

In the "filling-box" solution the entrainment volume per unit depth into the plume is assumed to be $2\pi REW$ at all depths. For an axisymmetic plume far from all side walls this provides us with the horizontal

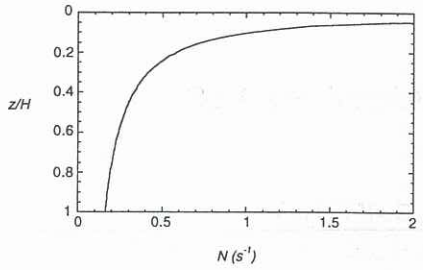

Figure 2. The "filling-box" buoyancy frequency N for an experiment in a 1.1 m × 0.3 m × 0.235 m tank where the source buoyancy flux is 6.81×10^{-7} m^{4}s^{-3}.

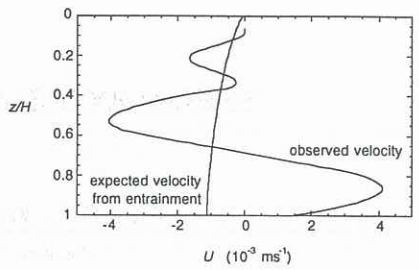

Figure 3. A sample horizontal velocity profile observed in an experiment compared with the velocity profile induced by entrainment only (3).

velocity directed radially into the plume. In the experiments reported below the plume is also placed near one end of a long channel in order to constrain the flow in the environment far from the plume to be two-dimensional. We assume that the entrained water is sourced evenly across the tank's horizontal cross-section so that the horizontal volume transport increases linearly from zero at the end of the tank opposite the plume to $2\pi REW$ at the plume's edge. Thus if B is the width, L the length of the tank and x the distance from the plume end, then the horizontal velocity U attributed to entrainment is

$$U = -2\pi ERW\frac{(L-x)}{BL}. \qquad (3)$$

The negative sign indicates that entrainment velocities are directed towards the plume. For the experiment described in figure 2, a plot of the expected entrainment-driven horizontal velocity profile (3) is given in figure 3.

EXPERIMENTS

In the experiments a dense salt solution was released at a steady rate through a small nozzle of a tank of water to approximate a pure buoyancy source. The nozzle, positioned near one end of the tank and equidistant from three side walls, protruded just below the free surface. A peristaltic pump maintained a constant flux of salt water through the nozzle.

Horizontal velocities far from the plume were measured by dropping crystals of potassium permanganate into the tank. As they descended to the bottom, the crystals dissolved to produce a vertical dye line. Horizontal velocities were calculated by measuring the distortion of this dye line in a short period of time. The short time interval was crucial to ensure the dye did not reach the end walls and also to minimise errors due to the simultaneous upwelling of the water. The movement of the dye line was recorded on video. A grid of lines with 1 cm spacing on the front of the tank allowed measurements of dye displacement correct to 0.5 cm from the video recording.

In addition to experiments starting with a homogenous tank that revealed the velocity structure at large times, twelve experiments were conducted to study the evolution of the flow starting from a plume-stratified tank at rest. A variety of tank sizes and source buoyancy fluxes were used in these experiments. In each case, the plume was run for up to four hours. Within the first hour the first front approached the level of the source and the density profile approached the asymptotic shape. After another three hours, the plume was turned off and the motions in the stratified tank allowed to settle to rest. The plume was then restarted and the subsequent redevelopment of the horizontal velocity profile monitored.

RESULTS

The circulation

The most striking observation was that the stratified environment produced by a turbulent plume supported a strong and persistent series of layers. These layers appeared as dominant features in the profiles of horizontal velocity, as seen in figures 1 and 3, but corresponded to extremely small perturbations in the density as it increased with time. (The density at a fixed point in the tank was measured using a conductivity probe, but is not shown here.) Hence we call these shear layers in order to distinguish them from density layering. At the bottom of the tank the outflow layer thickness was approximately one-quarter of the tank depth. Immediately above the outflow layer there was a layer of similar thickness moving towards the plume. In the upper half of the tank there were several layers. Both vertical scales and the magnitudes of the horizontal velocities in the shear layers generally decreased with height. At the centre of the third and fifth layers from the bottom, as defined by local velocity extrema, the water was almost stationary. Between these two layers there was a region of moderate flow towards the plume. At the third velocity extremum (z/H = 0.3 to 0.4), the velocity actually oscillated slowly from positive to negative, so that the flow was at times away from the plume.

At the end of the tank away from the plume, we also observed a concentrated upwards flow from the bottom outflow layer that fed the return flow towards the plume in the second layer. This existed because the uniform vertical advection distributed over the area of the box at the top of the outflow layer was insufficient to accommodate the total volume flux supplied to the layer by the turbulent plume. The same process continued to operate to some extent above the second

shear layer with a tendency for the horizontal volume flux in each layer to partly reflect from the end walls and return in the next layer.

It should be emphasised that water elements did not necessarily traverse the tank from end to end during their residence time in each layer. The distributed vertical advection of water "short-circuited" the paths. For example there was little horizontal flow (relative to the tank) in the third layer, yet if a thin layer of water was dyed, this dyed water was seen to migrate upwards through this layer. Thus those water particles which were not entrained into the plume migrated upwards through the series of shear layers, experiencing an oscillatory horizontal velocity.

Shear layer establishment

After the tank had been stratified the plume was turned off and the motions allowed to decay. The plume was later restarted and horizontal velocity profiles were taken at regular intervals. In twelve experiments, the pattern of development of the layers was the same. At small times the stratified water above the outflow layer began to move away from the plume and a broad region in the upper half of the box moved towards the plume. Ignoring the effects of stresses imposed by the rigid (no slip) bottom and the partly-rigid (free-slipping) surface at the top, this motion resembled the second baroclinic mode (see next section). The position of the inflow velocity maximum shifted down with time and a third shear layer soon formed at the top. We will see below that the motion at this stage appeared to be dominated by the third baroclinic mode. Additional vertical structure continued to develop in the velocity profile, consistent with the appearance of higher baroclinic modes being excited by the bottom outflow, until the velocity profile approached that of figure 3. The time required for the development of the baroclinic structure was only one-tenth the time required for the tank to be refreshed with the new plume water. The dominant vertical length scale of the velocity profile appeared to be set by the depth of the plume outflow. Physically, this is consistent with the outflow being the dominant, most energetic part of the system, with a well-defined vertical scale.

We estimated the time scale for establishment of the shear layers by measuring the time t_e taken for a four layered system to develop. A plot of t_e against the timescale for long internal waves to travel the length of the tank t_w, each normalised by $\overline{N}^{-1}$, appears in figure 4. The time for the development of the shear layers was proportional to the travel time of internal waves. The data are well described by a straight line passing through the origin, $t_e = (12.6 \pm 0.8)\ L/\overline{N}H$. Establishment timescales that are 12 to 15 times the $L/\overline{N}H$ scale are consistent with the dominance of higher baroclinic modes which have smaller phase speeds.

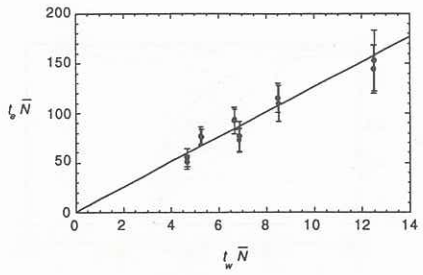

Figure 4. The time t_e taken for the velocity structure to evolve to a four layered system is proportional to t_w, the time scale for long internal waves to travel the length of the tank. Note that $t_w \overline{N} = L/H$.

BAROCLINIC NORMAL MODES

For the "filling-box" stratification (figure 2), the first eight baroclinic modes were calculated numerically, neglecting the effects of viscosity. We assume that these modal velocities are linearly superimposed on the entrainment-driven flow and the vertical advection of the environment. In this section, x is the distance along the tank, y the height from the bottom, u and w the usual velocities and $\rho_0(y)$ the density profile. We assume that a disturbance (plume outflow) at the bottom of the tank generates internal waves which propagate through the tank. The equations of motion in the two dimensional case are

$$\frac{\partial u}{\partial x} + \frac{\partial w}{\partial y} = 0,$$

$$\rho_0 \frac{\partial u}{\partial t} + \frac{\partial p'}{\partial x} = 0, \qquad (4)$$

$$\rho_0 \frac{\partial w}{\partial t} + \frac{\partial p'}{\partial y} + \rho' g = 0$$

and

$$\frac{\partial \rho'}{\partial t} + w \frac{d\rho_0}{dy} = 0,$$

where ρ' and p' are small perturbations of the density and pressure field respectively.

Following Gill (1982), w and p' can be separated into

$$w = \hat{h}(y)\tilde{w}(x,t) \quad \text{and} \quad p' = \hat{p}(y)\tilde{\eta}(x,t).$$

There is an infinite sequence of eigenfunctions (normal modes) that satisfy (4) and the relevant boundary conditions of a rigid, but free-slipping top and bottom. The solutions to $\hat{h}$ and $\hat{p}$ are calculated numerically. The zero-frequency horizontal velocity, which is applicable in infinitely long tanks, is proportional to $\hat{p}(y)/g\rho_0(y)$. The normalised horizontal velocity u for the first eight modes are given in figure 5 where we have converted the vertical axis to z/H. Note that in each mode, the integral of the horizontal velocity over the tank depth is zero, consistent with the assumption of no net volume flux away from or towards the plume.

The measured horizontal velocity profiles (figure 4) in the region $0.9 < z/H < 1$ are qualitatively similar to the velocity structures of the sixth, seventh and eighth inviscid modes except that the amplitudes of the horizontal velocities increase with height in the latter. In contrast, the structures of the lower modes (n = 1 to

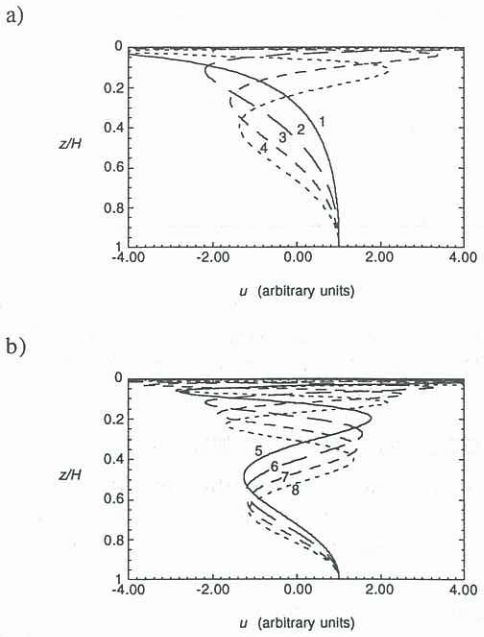

Figure 5. Inviscid baroclinic normal modes for the filling-box stratification. (a) The first four modes and (b) the next four modes.

4) were seen only at short times after the plume was started in the pre-established stratification. The observations were therefore consistent with the early appearance, particularly in the upper half of the water column, of the most rapidly propagating lower modes and with the later appearance of the slower propagating modes that were the most strongly excited. On the other hand, the measured horizontal velocities decay with height, whereas the calculated baroclinic modes have amplitudes that increase with height as a result of the nonlinear density gradient. The difference can be attributed to effects of viscous dissipation which acts most strongly on the smaller vertical scales characteristic of the higher baroclinic modes and of the upper, more highly stratified levels of the box (next section).

For finite tanks, the solution to (4) indicate that all horizontal velocities should oscillate in direction. The oscillation was not seen because the plume outflow maintains a constant flow in the bottom layer. Thus although the horizontal velocities are calculated for infinitely long tanks, they are also valid for finite tanks as well.

VISCOUS EFFECTS

We examine how viscosity modifies the baroclinic modes. Again we disregard the entrainment of water into the plume and the vertical advection of the environment. We assume that a disturbance at the bottom of the tank supplies the energy to develop and sustain the horizontal velocities of the baroclinc normal modes. The energy is transported vertically by waves propagated from the bottom while the momentum of the horizontal flow is slowly dissipated through viscous effects. If K is the kinetic energy per

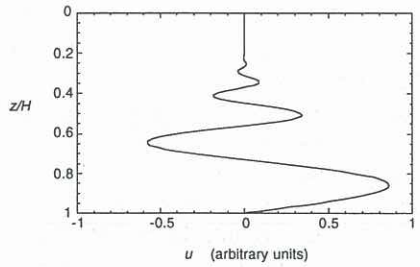

Figure 6. The normalised horizontal velocity u allowing for viscous dissipation of kinetic energy. The plot is for an experiment where the bottom outflow thickness is approximately one-quarter the total depth.

unit mass and c_g the energy propagation speed in the vertical then

$$\frac{DK}{Dt} = c_g \frac{\partial K}{\partial y} \approx -\rho_0 \upsilon \left(\frac{\partial u}{\partial y} \right)^2 .$$

When this is applied to the horizontal velocities of a normal mode, the velocities decay with distance from the bottom (figure 6) and more closely resemble the observed profile of figure 3. In the experiments, dissipation of momentum at the bottom would reduce the supply of momentum from the outflow layer, while dissipation at the side-walls would further contribute to losses in the upward propagating momentum.

CONCLUSION

The stratified environment produced by a turbulent plume supports a series of shear layers superimposed on the steady vertical advection and entrainment-driven horizontal flow into the plume. These layers are the result of a continuous excitation of baroclinic normal modes having vertical length scales set by the depth of the turbulent outflow from the dense plume. The horizontal velocities of these shear layers are large compared with the entrainment-induced and advection velocities, but have little effect on the stratification. The presence of the layers have major implications for the transport of water masses in filling-boxes.

REFERENCES

BAINES, W. D. and TURNER, J. S. "Turbulent buoyant convection from a source in a confined region." *J. Fluid Mech.* **37**, 51-80, 1969.

GILL, A.E. "Atmosphere-Ocean Dynamics", Academic Press, 1982.

TURNER, J.S. "Turbulent entrainment: the development of the entrainment assumption, and its application to geophysical flows." *J. Fluid Mech.* **173**, 431-471, 1986.

WONG A. B. D. and GRIFFITHS, R. W. "Shear layers driven by turbulent plumes." *J. Fluid Mech.* submitted, 1998.